Quasi-Self-Similar Evolution of the Two-Point Correlation Function: Strongly Nonlinear Regime in $\Omega_0 < 1$ Universes

Tatsushi Suginohara[1], Atsushi Taruya, and Yasushi Suto

Department of Physics and Research Center for the Early Universe, School of Science, University of Tokyo, Tokyo 113-0033, Japan.

tatsushi@res.otaru-uc.ac.jp, ataruya@utap.phys.s.u-tokyo.ac.jp, suto@phys.s.u-tokyo.ac.jp

ABSTRACT

The well-known self-similar solution for the two-point correlation function of the density field is valid only in an Einstein – de Sitter universe. We attempt to extend the solution for non – Einstein – de Sitter universes. For this purpose we introduce an idea of quasi-self-similar evolution; this approach is based on the assumption that the evolution of the two-point correlation is a succession of stages of evolution, each of which spans a short enough period to be considered approximately self-similar. In addition we assume that clustering is stable on scales where a physically motivated 'virialization condition' is satisfied. These assumptions lead to a definite prediction for the behavior of the two-point correlation function in the strongly nonlinear regime. We show that the prediction agrees well with N-body simulations in non – Einstein – de Sitter cases, and discuss some remaining problems.

Subject headings: cosmology: theory — large-scale structure of universe — gravitation — methods: N-body simulations

1. Introduction

It is generally believed that the structure in our universe has grown out of tiny density fluctuations through gravitational instability. The growth of those density fluctuations is

[1]Present address: Faculty of Commerce, Otaru University of Commerce, Otaru 047-8501, Japan.

completely described by linear theory on scales much larger than the correlation length of the density field (e.g., Peebles 1980). The behavior of the nonlinear density field on smaller scales, however, needs to be modeled with additional assumptions, and the resulting predictions should be verified and calibrated through extensive comparison with N-body simulations.

The most popular prediction in the nonlinear regime is based on the combination of the self-similar evolution and the stable clustering ansatz (Peebles 1974, 1980; Davis & Peebles 1977); if the linear power spectrum of density field follows a single power law $\propto k^n$, and the universe is described by the Einstein – de Sitter model, the evolution proceeds in a self-similar manner since there is no characteristic scale in the system. This self-similarity, together with the ansatz that the clustering is stable in the strongly nonlinear regime, predicts that the logarithmic slope of the two-point correlation function ξ is equal to $-3(n+3)/(n+5)$.

This solution has been widely applied in modeling the nonlinear gravitational clustering (Hamilton et al. 1991; Peacock & Dodds 1994, 1996; Jain, Mo & White 1995) and in understanding the pair-wise velocity dispersions and thus the redshift-space distortion (Suto & Jing 1997; Jing, Mo & Börner 1998). In fact, the above prescription has been applied even in the cases where the universe is not described by the Einstein – de Sitter model, and/or the linear power spectrum is not of a power-law form. The fitting formula for the nonlinear power spectrum by Peacock & Dodds (1996), for instance, takes account of the non power-law nature of the linear spectrum, but they have not examined the validity of the stable clustering solution in non Einstein – de Sitter models because 'if collapse occurs at high redshift, then $\Omega = 1$ may be assumed at that time' (Peacock & Dodds 1994).

We revisit this issue in detail for the non – Einstein – de Sitter case, i.e., when the matter density parameter Ω_0 is smaller than unity. Using N-body simulations with 64^3 particles, Suginohara et al. (1991) already found that while the stable solution is reproduced well in the Einstein de – Sitter model, the slope of ξ becomes steeper in $\Omega_0 < 1$ models (see also Suto 1993). This is not surprising at all because the derivation of the solution heavily relies on the scale-free nature of the Einstein – de Sitter model, that is, (1) $a \propto t^{2/3}$, where a is the cosmic scale factor, and (2) $D(t) \propto a$, where $D(t)$ is the linear growth rate of density fluctuations. This motivates us to find a suitable modification of the self-similar solution which is also applicable to the non – Einstein – de Sitter case.

In this paper we introduce an idea of quasi-self-similarity. This is based on the assumption that the evolution of the two-point correlation proceeds as a sequence of different quasi-self-similar stages, each of which is described by the *locally* self-similar solution determined by the cosmological parameters at that epoch. We also assume that the clustering becomes stable on scales where a 'virialization condition' is satisfied. These two assumptions lead to

a prediction of the behavior of the two-point correlation function in the strongly nonlinear regime. We show the extent to which the prediction agrees with the results of high-resolution N-body simulations.

2. Quasi-Self-Similar Evolution

2.1. The Self-Similar Solution in the Einstein–de Sitter Model

For later convenience, we first briefly review the self-similar solution in the Einstein–de Sitter case (Peebles 1974, 1980; Davis & Peebles 1977). Suppose a system of particles with mass m. In the fluid limit, the system is described by the one-particle distribution function $f(\mathbf{x},\mathbf{p},t)$, where $\mathbf{x}$ is the comoving coordinate, and $\mathbf{p} \equiv ma^2 d\mathbf{x}/dt$ is its canonical momentum. The distribution function $f(\mathbf{x},\mathbf{p},t)$ obeys the Vlasov equation (Inagaki 1976; Peebles 1980):

$$\frac{\partial f}{\partial t} + \frac{p_i}{ma^2}\frac{\partial f}{\partial x_i} - m\frac{\partial \phi}{\partial x_i}\frac{\partial f}{\partial p_i} = 0, \tag{1}$$

where the gravitational potential ϕ satisfies

$$\nabla^2 \phi = 4\pi G m a^{-1} \int f\, d^3p. \tag{2}$$

In the Einstein – de Sitter model ($a \propto t^{2/3}$), equation (1) admits a self-similar solution of the form:

$$f(\mathbf{x},\mathbf{p},t) = t^{-3\alpha-1} \hat{f}(\mathbf{x}/t^{\alpha}, \mathbf{p}/t^{\alpha+1/3}). \tag{3}$$

The value of the parameter α is determined by matching the solution in a linear regime as follows; first note that equation (3) implies the following form for the two-point correlation function $\xi(x,t)$:

$$\xi(x,t) = \hat{\xi}(x/t^{\alpha}). \tag{4}$$

If the initial power spectrum of density fluctuations, $P_{\mathrm{initial}}(k)$, is proportional to k^n, then $\xi(x,t)$ at later epochs behaves as $x^{-(n+3)}t^{4/3}$ on large scales where linear theory is valid. Thus the value of α is explicitly specified as

$$\alpha = \frac{4}{3(n+3)}. \tag{5}$$

In the small scale (nonlinear) limit, it is often assumed that the average proper separation of pairs remains constant (the stable clustering hypothesis):

$$\langle v_{21}(x,t)\rangle = -\dot{a}x, \tag{6}$$

where v_{21} is the relative peculiar velocity for a pair, and the brackets denote the average over pairs at a given comoving separation x. This assumption with equation (4) fixes the behavior of the correlation function in the nonlinear limit. Substituting equation (6) into the equation of the particle pair conservation:

$$\frac{\partial \xi}{\partial t} + \frac{1}{ax^2}\frac{\partial}{\partial x}[x^2(1+\xi)\langle v_{21}(x,t)\rangle] = 0, \tag{7}$$

yields

$$\frac{\partial \xi}{\partial t} = \frac{\dot{a}}{a}\frac{1}{x^2}\frac{\partial}{\partial x}[x^3\xi], \tag{8}$$

for $\xi \gg 1$. Thus ξ in the nonlinear regime should be of the form

$$\xi = a^3 g(ax), \tag{9}$$

where g is an arbitrary function at this point. Finally the consistency with the above similarity solution requires that ξ should be given by the following power-law form:

$$\xi(x,t) \propto x^{-\frac{3(n+3)}{n+5}}\, t^{\frac{4}{n+5}} \propto x^{-\frac{3(n+3)}{n+5}}\, a^{\frac{6}{n+5}}. \tag{10}$$

2.2. Quasi-Self-Similar Clustering Solutions

Now we attempt to generalize the above self-similar solution in a hypothetical universe where $a \propto t^p$ and $D(t) \propto t^q$. In non–Einstein–de Sitter models, both p and q are not constant but change with time. As long as the time-scale of the change of p and q is smaller than that of the cosmic expansion, however, they can be regarded as constants for a short period at each epoch.

We begin with the assumption of similarity for $\xi(x,t)$:

$$\xi(x,t) = \hat{\xi}(x/t^{\alpha}). \tag{11}$$

Unlike in the Einstein – de Sitter case, any kind of self-similarity does not hold in a strict sense. However, the range of p and q considered here is close to that in the Einstein – de Sitter case, so it seems reasonable to assume that some form of self-similarity is realized

in an approximate sense. The simplest possibility is that, as in the previous subsection, $\xi(x,t)$ has the form (11). With this ansatz we repeat the same procedure in the previous subsection, adopting $P_{\rm initial}(k) \propto k^n$ and the stable clustering hypothesis in the strongly nonlinear regime.

In this case, one has $\xi \propto x^{-(n+3)} t^{2q}$ in linear regime, and equation (5) is replaced by

$$\alpha = \frac{2q}{n+3}. \tag{12}$$

Combining the form (9) for ξ in the strongly nonlinear regime yields, instead of equation (10),

$$\xi(x,t) \propto x^{-\frac{3(n+3)}{n+3+2f}} \, a^{\frac{6f}{n+3+2f}} = (ax)^{-\frac{3(n+3)}{n+3+2f}} \, a^3, \tag{13}$$

for $\xi \gg 1$. The quantity $f \equiv q/p$ in the above expression is in fact the familiar logarithmic derivative of D with respect to a. An excellent approximation to f is (Lahav et al. 1991)

$$f = \frac{d \ln D}{d \ln a} \sim \Omega(a)^{0.6} + \frac{\lambda(a)}{70} \left[1 + \frac{\Omega(a)}{2} \right], \tag{14}$$

where

$$\Omega(a) = \frac{\Omega_0}{\Omega_0 + (1 - \Omega_0 - \lambda_0)(a/a_0) + \lambda_0 (a/a_0)^3} \tag{15}$$

and

$$\lambda(a) = \frac{\lambda_0 (a/a_0)^3}{\Omega_0 + (1 - \Omega_0 - \lambda_0)(a/a_0) + \lambda_0 (a/a_0)^3}, \tag{16}$$

with λ_0 being the dimensionless cosmological constant at the present epoch a_0.

2.3. Comparison with N-body Simulations

Let us compare in detail the self-similar solution (eq. [10]) and the quasi-self-similar solution (eq. [13]) with high-resolution N-body simulations (Jing 1998; 2001b in preparation). The simulations consist of two Einstein – de Sitter models, two open models ($\Omega_0 = 0.1$, $\lambda_0 = 0$), and two spatially flat models ($\Omega_0 = 0.1$, $\lambda_0 = 0.9$). All the models employ scale-free initial power spectra $P_{\rm initial}(k) \propto k^n$ with $n = -1$ and $n = -2$. Gravitational force calculation is based on the $\mathrm{P^3M}$ algorithm. Simulation parameters are listed in Table 1, and further details of the simulations are described in Jing (1998, 2001b in preparation).

Figure 1a plots the two-point correlation functions which are appropriately scaled with respect to x according to the conventional self-similar solution (eq.[10]). It is clear that while $\Omega_0 = 1$ simulations are in good agreement with equation (10) beyond $\xi = 100$ (indicated by an arrow for each model), $\Omega_0 = 0.1$ models are not; the disagreement is particularly severe for the $\lambda_0 = 0$ models. Figure 1b shows the similar plot but with scaling for quasi-self-similar solution (eq.[13]), where we use the value of f evaluated at the present epoch. The figure indicates that the agreement with the simulations in $\Omega_0 = 0.1$ models indeed improves. Nevertheless the results in $\Omega_0 = 0.1$ and $\lambda_0 = 0.9$ models do not yet show acceptable agreement with equation (13). The origin of the disagreement is studied by Suto, Taruya, & Suginohara (2001).

This comparison points to the following two suggestions; (i) in $\Omega_0 < 1$ models the conventional self-similar solution fails to describe the behavior of ξ for $\xi \gtrsim 100$, and (ii) taking account of the dependence of the slope on the cosmological parameters as in equation (13) does not yet yield an acceptable prediction. With these points in mind we attempt to improve the quasi-self-similar solution in the next section.

3. An Improved Model

3.1. Virialization Condition and Scale Dependence of the Slope of ξ

In the previous section we have applied the quasi-self-similarity only at the present epoch. In reality, however, the logarithmic slope of the correlation function:

$$\frac{d\ln\xi}{d\ln x} = -\frac{3(n+3)}{n+3+2f(a_{\rm vir}(x))} \tag{17}$$

should be fixed locally at the epoch of the virialization of the corresponding scale, $a_{\rm vir}(x)$. This naturally generates additional scale-dependence on the resulting solution through the time-dependence of f. More specifically, we attempt to incorporate this effect and to improve the model in the previous subsection as follows.

In order to determine $a_{\rm vir}(x)$ at each scale x, we need to make an assumption about the scale on which the system has been virialized at a given epoch a. Here we mainly adopt the following assumption: the system has just been virialized at a scale $x_{\rm vir}(a)$ where the volume average of the two-point correlation function reaches the critical overdensity of a virialized halo, $\Delta_{\rm vir}(a)$, predicted by the spherical collapse model:

$$\bar{\xi}(x_{\rm vir}(a)) = \Delta_{\rm vir}(a), \tag{18}$$

where

$$\bar{\xi}(x) \equiv \frac{3}{x^3}\int_0^x y^2\xi(y)dy. \tag{19}$$

It seems natural to use $\bar{\xi}$ rather than ξ for the present purpose because the right-hand-side of equation (18) is the *average* density of a halo that has just been virialized. In $\lambda_0 = 0$ models, the critical density $\Delta_{\rm vir}(a)$ is explicitly written as (Lacey & Cole 1993)

$$\Delta_{\rm vir}(a) = 4\pi^2\frac{(\cosh\eta - 1)^3}{(\sinh\eta - \eta)^2}, \tag{20}$$

$$\cosh\eta = \frac{2}{\Omega(a)} - 1, \tag{21}$$

and its accurate fitting formula in $\lambda_0 = 1 - \Omega_0$ models (Nakamura & Suto 1997) is given by

$$\Delta_{\rm vir}(a) \simeq 18\pi^2\left\{1 + 0.4093\left[\frac{1}{\Omega(a)} - 1\right]^{0.9052}\right\}. \tag{22}$$

The 'virialization condition' (18) may be somewhat arbitrary, but is perhaps most natural and physically motivated among other choices.

Furthermore we assume that, for $x \le x_{\rm vir}(a)$, the stable clustering condition is satisfied, i.e., $\xi(x,a)$ is of the form (9). This is equivalent to saying that, at a fixed physical scale $r = ax$, the slope of ξ is kept constant while its amplitude grows in proportion to a^3 (c.f., eq.[13]).

The above assumptions are not yet sufficient in predicting $\xi(x)$ for a given model. The amplitude of ξ at an arbitrary point needs to be specified by hand because our model does not predict the overall amplitude of $\xi(x)$. Once the value of ξ is fixed at a scale $x = \varepsilon$ (for example, in the next subsection, we take $\varepsilon_{\rm grav}$, the gravitational softening length, as ε and use the value of $\xi(\varepsilon_{\rm grav})$ in the simulations), we can compute $\xi(x)$ at $a = a_0$ up to $x_{\rm vir,0} \equiv x_{\rm vir}(a_0)$. The procedure is as follows:

1. *Set boundary condition.* — Below an extremely small scale x_l, where ξ is sufficiently large, our model prediction should reduce to the conventional self-similar solution in the Einstein – de Sitter universe; i.e.,

$$\xi \propto x^{-3(n+3)/(n+5)} \qquad \text{for } x \le x_l. \tag{23}$$

This is because the epoch of the virialization of the corresponding scale is sufficiently early, the universe is indistinguishable from the Einstein – de Sitter model (Peacock & Dodds 1994). Equation (23) implies that

$$\bar{\xi}(x_l) = \frac{(n+5)}{2}\xi(x_l). \tag{24}$$

We first choose x_l arbitrarily and set the value of $\xi(x_l)$ to be sufficiently large, say, 10^8. This is the starting point of our computation.

2. *Compute* $a_{\rm vir}(x)$. — From the above assumptions it follows that

$$\bar{\xi}(x) = \left(\frac{a_{\rm vir}(x)}{a_0}\right)^{-3} \Delta_{\rm vir}(a_{\rm vir}(x)). \quad (25)$$

At the current scale x, we solve equation (25) for $a_{\rm vir}(x)$.

3. *Advance* x . — Substituting the value of $a_{\rm vir}(x)$ into equation (17) gives the local slope $d\ln\xi/d\ln x$ at x. Then we can advance x by a small interval Δx and compute $\xi(x+\Delta x)$, and then $\bar{\xi}(x+\Delta x)$.

4. We repeat the procedures 2 and 3 until $\bar{\xi}(x)$ becomes equal to $\Delta_{\rm vir}(a_0)$, which corresponds to the present virialization scale $x_{\rm vir,0}$.

5. *Normalization.* — Finally we shift the resulting solution so that it can match the given amplitude at $x = \varepsilon$, using the fact that, if $\xi^{(1)}(x)$ is a solution to equation (17), so is $\xi^{(2)}(x) \equiv \xi^{(1)}(\alpha x)$ with an arbitrary constant α.

3.2. Comparison with N-body Simulations

Figure 2 compares our improved model predictions with the N-body results. Using the scaling relation described above, we match the amplitude of our solution to that of the simulations at $x = \varepsilon_{\rm grav}$ for each model (the innermost symbols). The length scale x is normalized by $x_{\rm vir,0} \equiv x_{\rm vir}(a_0)$ and we show the results only in the virialized regime, $x < x_{\rm vir,0}$. Clearly, our predictions are in good agreement with simulations for $\xi \gtrsim 200$ in all models. In particular the predicted dependence on the spectral index n is excellently reproduced in the simulation results. Given the simplicity of our procedure, this may be regarded as a considerable success. For $\xi < 200$, however, the slopes of our predicted correlation functions are shallower than those of simulations (Figs. 2a and 2b).

Let us compare our model predictions with the conventional self-similar solution (eq. [10]) in more detail. The power-law slope of the conventional self-similar solution is shown by the dot-dashed lines in Figure 2. In $\Omega_0 = 0.1$ and $\lambda_0 = 0.9$ cases both our model and the simulation have roughly the same slope as the conventional one near $x = \varepsilon_{\rm grav}$, but in both of them the slope becomes steeper as the scale approaches to $x_{\rm vir,0}$. More impressively, in $\Omega_0 = 0.1$ and $\lambda_0 = 0.0$ cases both our model and the simulation have a steeper slope on all scales shown in the figure than the conventional one.

Also shown in Figure 2 are the correlation functions obtained by Fourier-transforming

the fitting formulae for the nonlinear power spectra by Peacock & Dodds (1996). The Peacock-Dodds formula is extremely useful because it gives not only the shape but also the amplitude of the two-point correlation function from linear to strongly nonlinear regimes. The agreement between the Peacock-Dodds formula and the simulations is very well except for $\Omega_0 = 0.1$ and $\lambda_0 = 0$ models. In these cases the Peacock-Dodds formula systematically underpredicts the simulation results. Nevertheless this could be adjusted somehow by shifting the amplitude of the Peacock-Dodds formula so as to match the simulation at $x = \varepsilon_{\rm grav}$ (see the dotted lines in Fig. 2). Rather an important advantage of our model over the Peacock-Dodds prescription is that it does successfully *predict* the slope of ξ up to a scale where deviation from the conventional one, $-3(n+3)/(n+5)$, is significant. Note that the slope of ξ computed from the Peacock-Dodds formula is, on scales where it deviates from $-3(n+3)/(n+5)$, simply an interpolation from the numerical simulations. In this sense, our result implies that there is room for further improvement in the original Peacock-Dodds formula, and our present model may be useful for that purpose.

One may wonder if it is possible to improve our model predictions by varying the condition (18) somehow. Figures 3 and 4 present those results. The top panels in those figures adopt $\bar{\xi}(x_{\rm vir}(a)) = 2\Delta_{\rm vir}(a)$ instead of equation (18). While the agreement between the quasi-self-similar prediction and the simulations is indeed improved for $\Omega_0 = 1$ models, this is not the case for $\Omega_0 < 1$ models.

The middle and bottom panels show the results for $\xi(x_{\rm vir}(a)) = 100$, and $\bar{\xi}(x_{\rm vir}(a)) = 300$, respectively, instead of equation (18). In each case we obtain acceptable agreement for both $\Omega_0 = 1$ and $\Omega_0 < 1$ models simultaneously, although the modified conditions lose the physical basis and should be regarded as empirical at best.

3.3. Validity of the stable clustering hypothesis

The stable clustering hypothesis is an essential ingredient in our model, but has somewhat been in doubt in the recent literature (Yano & Gouda 2000; Ma & Fry 2000; Caldwell et al. 2001). We argue here, nevertheless, that the hypothesis still remains to be a reasonable assumption.

Yano & Gouda (2000) relate the inner density profile of virialized halos with the velocity parameter $h \equiv -\langle v_{21}\rangle/\dot{a}x$. They claim that h should approach zero in the nonlinear limit if the logarithmic slope of the inner density profile is larger than $-3/2$. As pointed out by Ma & Fry (2000), their argument is valid only when all halos have an equal mass, and should be completely altered for a realistic mass function.

On the basis of simulations by Jain (1997), Caldwell et al. (2001) find for a variety of cosmological models a universal relation between $f\bar{\xi}$ and h, and propose a fitting formula describing the relation. Although extrapolating this formula implies that $h \to 0$ in the nonlinear limit, they claim that their formula is valid for $f\bar{\xi} \lesssim 10^3$. Thus their results are not inconsistent with the idea that $h \sim 1$ in the strongly nonlinear regime. In fact, more recent numerical work supports the stable clustering assumption (Jing 2001a; Fukushige & Suto 2001).

4. Discussion

We have shown that the conventional self-similar solution in the Einstein – de Sitter universe does not describe the behavior of two-point correlation functions in $\Omega_0 \neq 1$ models for strongly nonlinear regimes of cosmological interest, $\xi < 10^4$. Instead, we have proposed a simple model to describe the two-point correlation functions in strongly nonlinear regimes by introducing the quasi-self-similar ansatz. In fact we have shown that the resulting model predictions in non – Einstein – de Sitter universes agree better with the high-resolution N-body simulations.

On the other hand, our current model is not fully successful yet in the sense that the predicted behavior for $\xi < 200$ systematically differs from that observed in simulations. Empirically this situation can be improved by an appropriate choice of the virialization threshold $\bar{\xi}_{\rm vir}$. While the physical meaning of this procedure is not clear, this may be related to some other physics that we omit in the present simple prescription. After all the regime for $\xi < 200$ may not be completely dominated by the stable clustering evolution, and the effect of linear and quasi-linear evolution is likely to be important as well. In fact it may be the case that the stable condition (6) is not realized instantaneously when the virial condition (18) is satisfied, and that the slope at the corresponding scale approaches the value implied by equation (17) only gradually as the scale becomes more strongly nonlinear (for instance, $\xi > 200$) and completely decoupled from the linear evolution of the environment. We plan to check this interpretation using the time-evolution of the simulation results in due course.

One of the most important applications of the conventional self-similar solution is the fitting formula for the nonlinear power spectrum by Peacock & Dodds (1996), which is based on an idea originally proposed by Hamilton et al. (1991). In the strongly nonlinear regime, on which we focus in this paper, the Peacock-Dodds formula agrees well with the simulations for $\Omega_0 = 1$, and also for $\Omega_0 < 1$ and $\Omega_0 + \lambda_0 = 1$. We have found, however, that in $\Omega_0 = 0.1$ and $\lambda_0 = 0$ cases the formula fails to fit the simulations. This may be understood as follows. In such cases the slope of ξ asymptotically approaches that in conventional self-

similar solution only on scales where ξ is extremely large. This means that the gap between these asymptotic scales and linear scales is rather big, and it cannot be simply interpolated. In contrast our model predicts the shape of ξ up to the scale corresponding to $\xi \sim$ a few hundred, so interpolation between this scale and the linear scale may be much easier. Thus our model may be useful in improving the Peacock-Dodds formula, especially in $\Omega_0 < 1$ and $\lambda_0 = 0$ cases.

In summary, although our proposed model still needs to be improved, the degree of success for $\xi \gtrsim 200$ is encouraging, and useful at least empirically. We hope that the idea of quasi-self-similar evolution may give a useful insight towards a better understanding of nonlinear dynamics of the mass density field in the universe. In particular, we plan to improve the existing fitting formula for the nonlinear power spectrum (Peacock & Dodds 1994, 1996) by applying the quasi-self-similar ansatz.

We are grateful to Y. P. Jing for kindly providing his results of N-body simulations. A. T. acknowledges support from Research Fellowships of the Japan Society for the Promotion of Science. This research was supported in part by the Grant-in-Aid by the Ministry of Education, Science, Sports and Culture of Japan (07CE2002, 12640231) to RESCEU, and by the Supercomputer Project (No.99-52, No.00-63) of KEK.

REFERENCES

Caldwell, R. R., Juszkiewicz, R., Steinhardt, P. J., & Bouchet, F. R. 2001, ApJ, 547, L93

Davis, M. & Peebles, P. J. E. 1977, ApJS, 34, 425

Fukushige, T. & Suto, Y. 2001, ApJ, 557, L11

Hamilton, A. J. S., Kumar, P., Lu, E. & Matthews, A. 1991, ApJ, 374, L1

Inagaki, S. 1976, PASJ, 28, 77

Jain, B. 1997, MNRAS, 287, 687

Jain, B., Mo, H. J. & White, S. D. M. 1995, MNRAS, 276, L25

Jing, Y. P. 1998, ApJ, 503, L9

Jing, Y. P. 2001a, ApJ, 550, L125

Jing, Y. P., Mo, H. J. & Börner, G. 1998, ApJ, 494, 1

Lacey, C. & Cole, S. 1993, MNRAS, 262, 627

Lahav, O., Rees, M. J., Lilje, P. B. & Primack, J. R. 1991, MNRAS, 251, 128

Ma, C.-P. & Fry, J. N. 2000, ApJ, 538, L107

Nakamura, T. T. & Suto, Y. 1997, Prog. Theor. Phys., 97, 49

Peacock, J. A. & Dodds, S. J. 1994, MNRAS, 267, 1020

Peacock, J. A. & Dodds, S. J. 1996, MNRAS, 280, L19

Peebles, P. J. E. 1974, ApJ, 189, L51

Peebles, P. J. E. 1980, The Large-Scale Structure of the Universe (Princeton: Princeton Univ. Press)

Suginohara, T., Suto, Y., Bouchet, F. R. & Hernquist, L. 1991, ApJS, 75, 631

Suto, Y. 1993, Prog. Theor. Phys., 90, 1173

Suto, Y. & Jing, Y. P. 1997, ApJS, 110, 167

Suto, Y., Taruya, A. & Suginohara, T. 2001, Progress in Astronomy (Supplement), 19, 67

Yano, T. & Gouda, N. 2000, ApJ, 539, 493

This preprint was prepared with the AAS LaTeX macros v5.0.

Table 1. Simulation parameters.

Ω_0	λ_0	n	N [a]	$\varepsilon_{\rm grav}/L_{\rm box}$ [b]
1.0	0.0	-1, -2	256^3	5.9×10^{-4}
0.1	0.0	-1, -2	200^3	7.5×10^{-4}
0.1	0.9	-1, -2	200^3	7.5×10^{-4}

[a]The number of particles.
[b]Gravitational softening length in units of the box size $L_{\rm box}$.

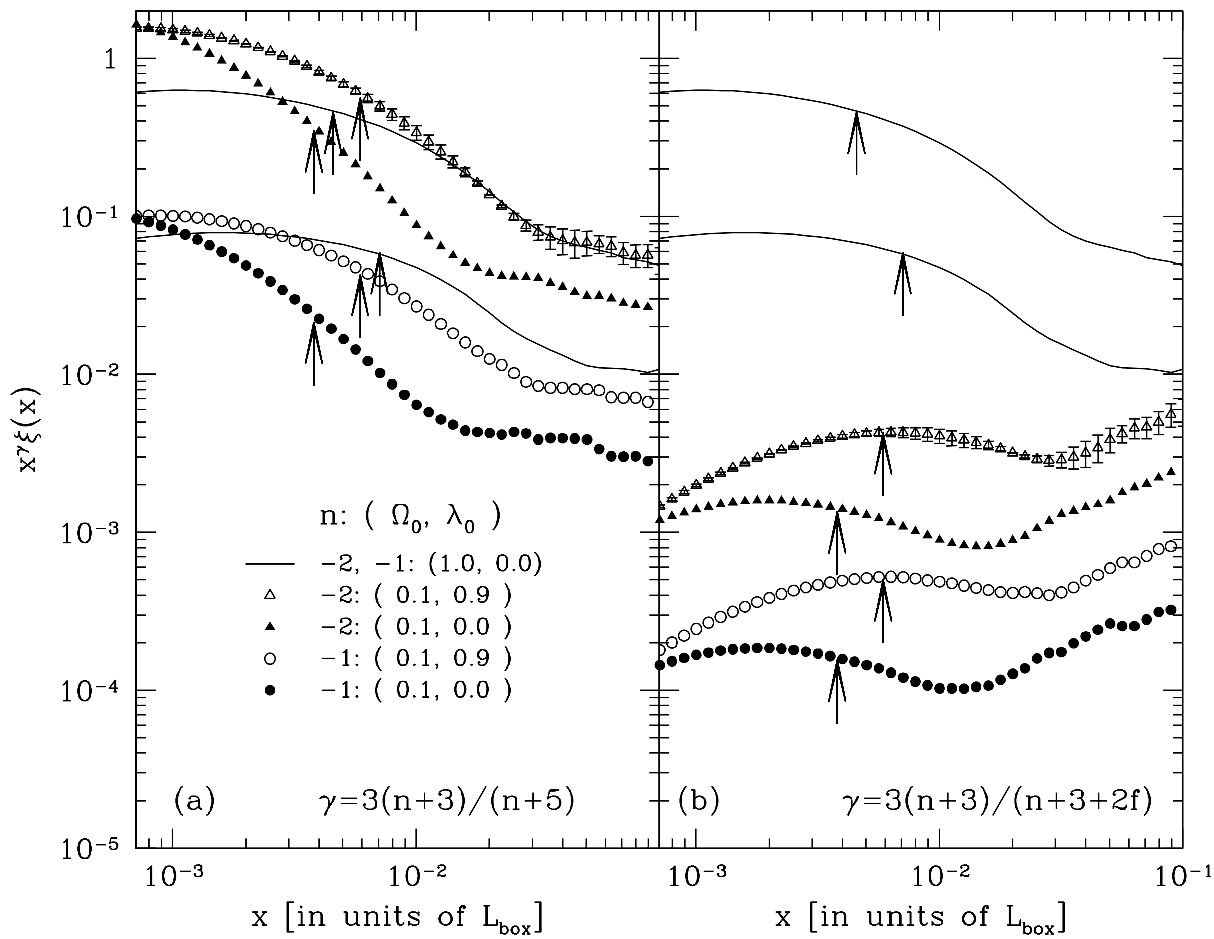

Fig. 1.— Two-point correlation functions in the simulations scaled according to (a) conventional self-similar solution, and (b) quasi-self-similar solution with scale independent slope. The solid lines are the results for $\Omega_0 = 1$ models, and the symbols are those for $\Omega_0 = 0.1$ models with either $\lambda_0 = 0$ or $\lambda_0 = 0.9$. Error bars are estimated from three realizations for each model; only the error bars for $n = -2$ and $(\Omega_0, \lambda_0) = (0.1, 0.9)$ are shown. Other models have smaller error bars, which are not shown for clarity. The arrows correspond to $\xi(x) = 100$ for each model.

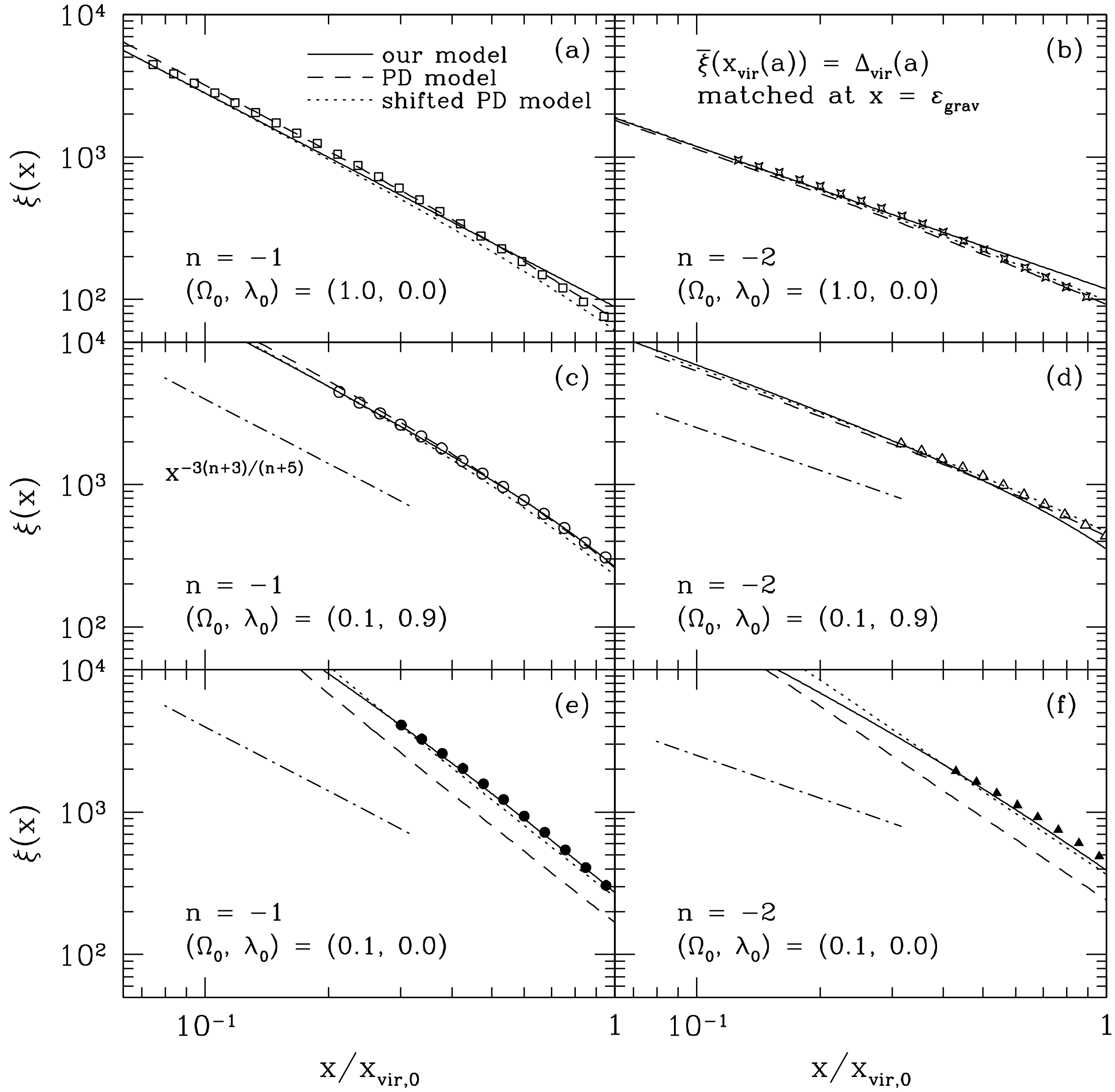

Fig. 2.— Quasi-self-similar solutions with a virialization condition $\bar{\xi}(x_{\rm vir}(a)) = \Delta_{\rm vir}(a)$. The solid lines are obtained by numerically integrating eq. [17]. The length scale x is normalized by $x_{\rm vir,0}$. The dashed lines are computed using the Peacock-Dodds formula. The dotted lines also show the Peacock-Dodds formula, but this time each result has been horizontally shifted to match the simulation at $x = \varepsilon_{\rm grav}$. The dot-dashed lines show the slope of the conventional self-similar solution. The symbols are the results of the simulations. (a) $n = -1$ and $(\Omega_0, \lambda_0) = (1.0, 0.0)$. (b) $n = -2$ and $(\Omega_0, \lambda_0) = (1.0, 0.0)$. (c) $n = -1$ and $(\Omega_0, \lambda_0) = (0.1, 0.9)$. (d) $n = -2$ and $(\Omega_0, \lambda_0) = (0.1, 0.9)$. (e) $n = -1$ and $(\Omega_0, \lambda_0) = (0.1, 0.0)$. (f) $n = -2$ and $(\Omega_0, \lambda_0) = (0.1, 0.0)$.

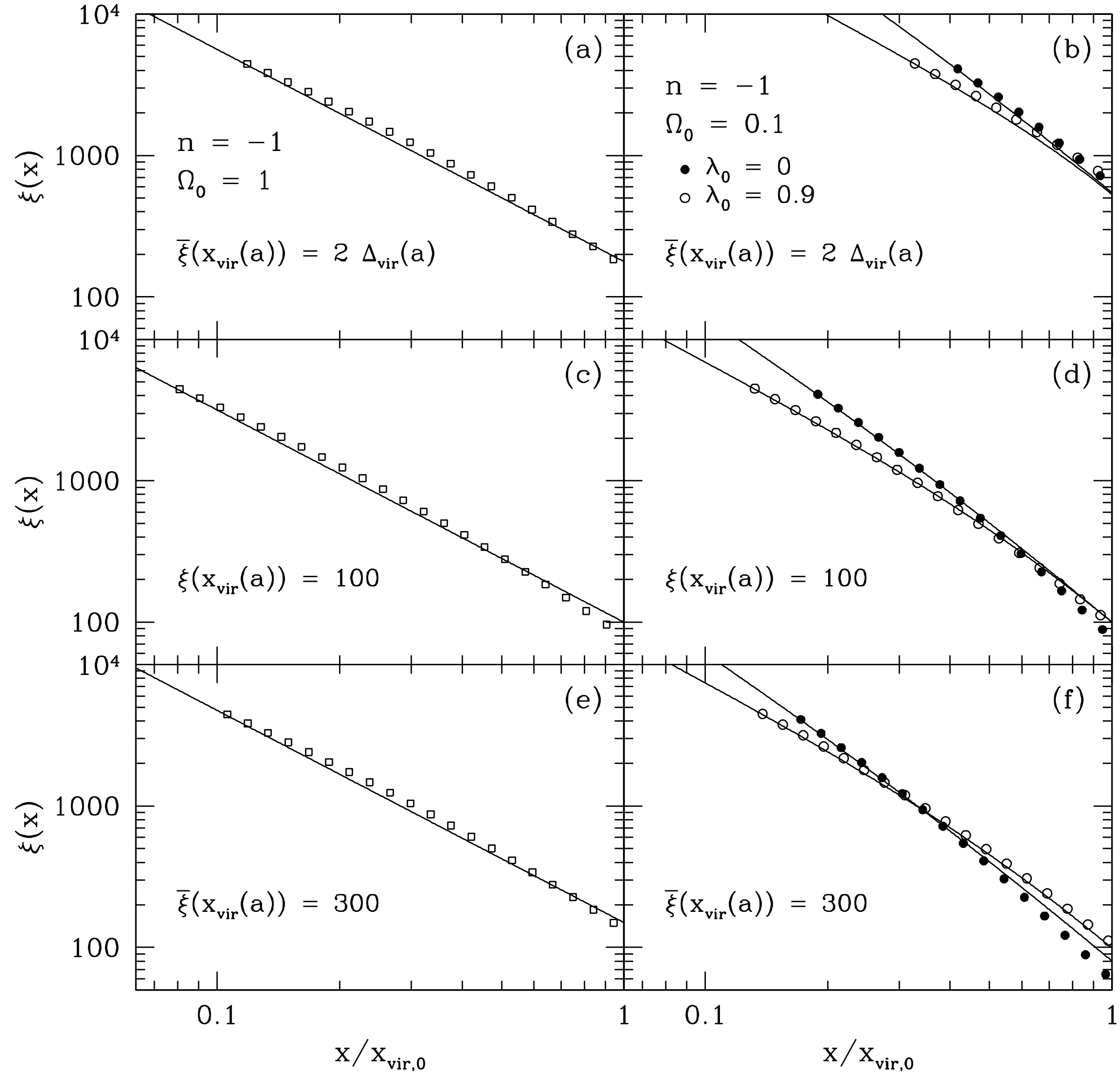

Fig. 3.— Quasi-self-similar solutions for $n = -1$. The solid lines are obtained by numerically integrating eq. [17]. The symbols are the results of the simulations. (a) $\Omega_0 = 1$ model with a virialization condition $\bar{\xi}(x_{\rm vir}(a)) = 2\Delta_{\rm vir}(a)$. (b) $\Omega_0 < 1$ models with $\bar{\xi}(x_{\rm vir}(a)) = 2\Delta_{\rm vir}(a)$. (c) $\Omega_0 = 1$ model with $\xi(x_{\rm vir}(a)) = 100$. (d) $\Omega_0 < 1$ models with $\xi(x_{\rm vir}(a)) = 100$. (e) $\Omega_0 = 1$ model with $\bar{\xi}(x_{\rm vir}(a)) = 300$. (f) $\Omega_0 < 1$ models with $\bar{\xi}(x_{\rm vir}(a)) = 300$.

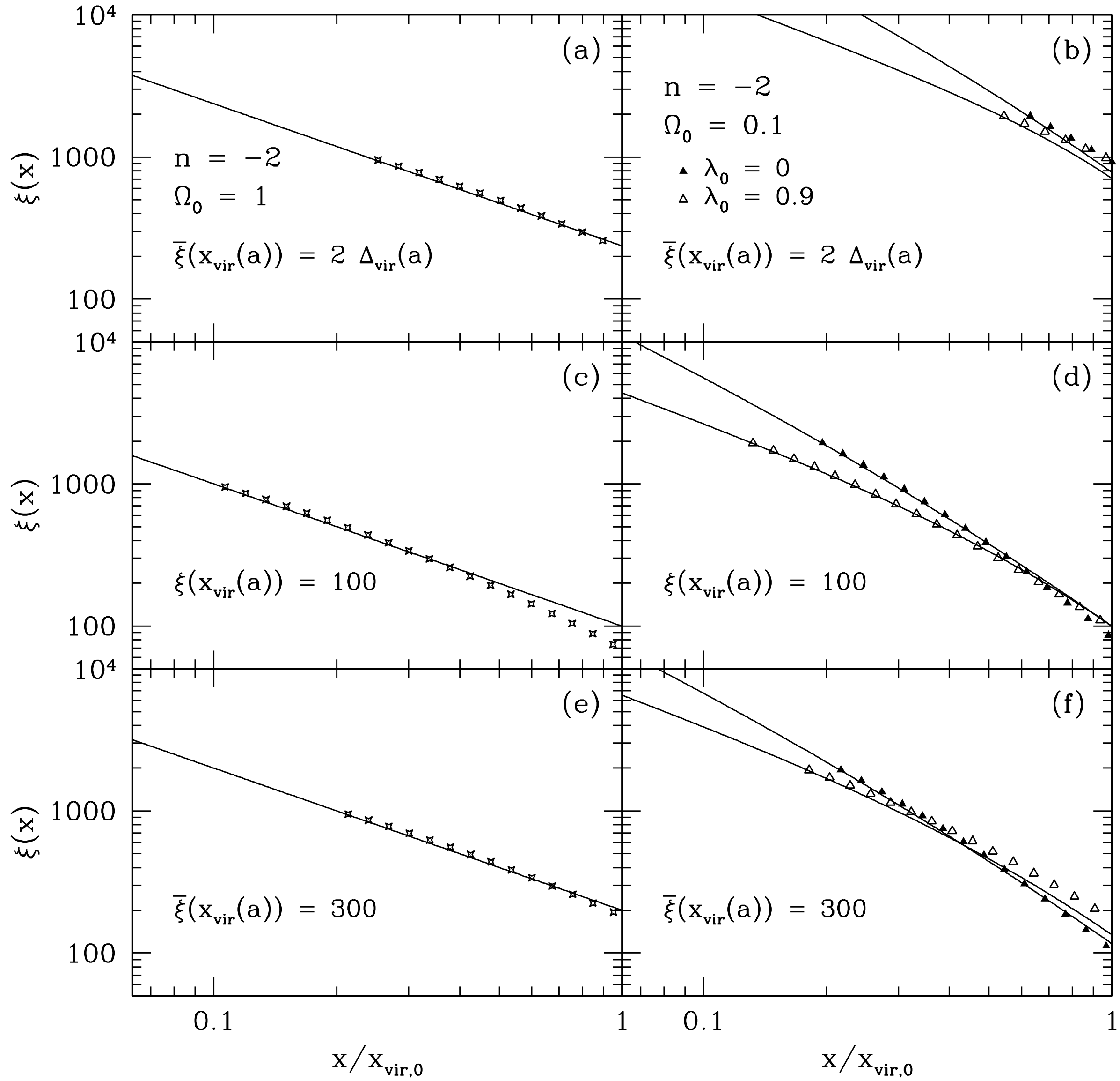

Fig. 4.— As for Fig. 3, but for $n = -2$.